



---

# TECHNICAL RESEARCH REPORT

## Optical Area-Based Surface Quality Assessment for In-Process Measurement

*by D.L. DeVoe and G.M. Zhang*

T.R. 93-60

*The Institute for Systems Research is supported by the  
National Science Foundation Engineering Research Center Program (NSFD CD 8803012),  
the University of Maryland, Harvard University, and Industry*

---

---

## OPTICAL AREA-BASED SURFACE QUALITY ASSESSMENT FOR IN-PROCESS MEASUREMENT

Don L. DeVoe and Guangming Zhang

Department of Mechanical Engineering and Institute for Systems Research  
University of Maryland  
College Park, MD

### ABSTRACT

The measurement of surface finish has been recognized as an important element of Computer Integrated Manufacturing (CIM) systems which perform on-line machining systems control. Optical methods for the in-process measurement of surface roughness have been developed for this purpose, but these systems have in many cases introduced excessive complexity in the CIM system. This work presents an area-based surface characterization technique which applies the basic light scattering principles used in other optical measurement systems. These principles are applied in a novel fashion which is especially suitable for in-process measurement and control. A prototype of the optical system to implement these principles is developed in this work. The experimental results are presented to demonstrate the capabilities and future potential for integrating the measurement system into a machining process to achieve significant improvement of quality and productivity.

### NOMENCLATURE

A	Surface area illuminated by incident light ( $A = X_s Y_s$ )
$F_i$	Frequency count of all pixels in an image
$R_a$	Average roughness
$R^2$	Correlation Coefficient
T	Statistical correlation distance between peaks on the surface, as defined by Beckmann (1963)
X, Y, Z	Global coordinates (relative to overall surface)
$X_s, Y_s$	x, y dimensions of a surface area A illuminated by the incident radiation
x, y, z	Local coordinates (relative to a surface facet)
$x_i$	Brightness level ( $0 \leq i \leq 255$ )
$\alpha$	Horizontal orientation of light source with respect to machining direction
$\gamma$	Angle of incidence (global)
$\lambda$	Wavelength of incident radiation
$\mu$	Mean histogram level

$\Omega$	Optical roughness parameter ( $\Omega = \mu/\sigma$ )
$\sigma$	Standard deviation of histogram
$\sigma_h$	Standard deviation of surface height
$\theta_1$	Angle of incidence (local)
$\theta_2$	Vertical angle of observation (local)
$\theta_3$	Horizontal angle of observation (local)
$\Psi$	Mean scattered power

### INTRODUCTION

Surface finish is vital to the performance and basic function of a broad range of industrial products, and the measurement of surface finish on the shop floor has been an important element of many quality control programs. The traditional methods of surface roughness assessment employed in these quality control programs have proven successful for the task of off-line surface measurement. However, there is a need for high-speed in-process measurement devices applicable to CIM systems which can measure the surface roughness during a machining process. Such a system should provide appropriate feedback to the process to ensure that the machined surface finish remains within desired tolerances. In-process inspection systems are necessary for the automatic control of surface quality in a sensor-based manufacturing environment.

Currently available methods of surface measurement suffer from a number of disadvantages which limit their application to in-process measurement schemes. Traditional methods of profilometry, such as stylus devices, require direct contact with the surface, thus limiting measurement speed, requiring navigation around surface discontinuities, and allowing environmental vibration to introduce significant noise into the measurements. Several non-contact measurement methods have been proposed to avoid the problems associated with stylus devices, such as laser-based profilometry devices and linear diode arrays, which can achieve much faster measurement speeds than stylus profilometers (Jansson, 1984). However, these optical

methods perform their measurement over a very limited area of the surface (either a point or line), and thus they require multiple measurements to accurately characterize a region of the surface large enough to provide adequate information regarding the overall surface topography. Such systems can be said to measure local surface roughness, as opposed to area-based systems which are capable of measuring the global surface roughness. In the case of many laser-based profilometry systems, multiple measurements over a range of incident and observation angles are required to determine the local roughness from a single point on the surface. The optical method proposed in this work employs an extension of the same theoretical framework used in these other optical systems, but it avoids many of the disadvantages associated with stylus devices, and it is capable of yielding roughness information from a large region of the surface in a single measurement, thus obviating the need for multiple single-point or line measurements across the surface as required with other optical measurement techniques.

In this paper, we present our efforts in implementing an optical area-based surface quality assessment technique. A theoretical basis which describes the operation of the technique was developed, and we designed and constructed a prototype vision system. A medium resolution charge coupled device (CCD) camera is used to capture a 490 x 510 pixel grayscale image of a rough surface illuminated by a light source. Basic image analysis is performed on the image to derive an optical roughness parameter as a performance index. The optical parameter can then be used to determine the average roughness of the machined surface. This paper is organized as follows: the theoretical background which describes the behavior of the system will be presented, followed by a detailed description of the system's hardware, and a discussion of several performance issues.

## APPLICATION OF OPTICAL SCATTERING

Many of the optical surface roughness measurement systems currently available apply the results of a light-scattering theory described in a monograph by Beckmann (1963). The theory states that the mean scattered power ( $\Psi$ ) of incident light is a function of surface roughness, incident wavelength, incident angle, observation angles, correlation distance between the hills or valleys in the surface, and planar dimensions of the illuminated surface. The equation describing this relationship is given by Beckmann as

$$\Psi = e^{-8} \left[ \rho_0^2 + \frac{\pi F T^2}{A} \sum_{m=1}^{\infty} \frac{g^m}{m!m} \exp\left(\frac{-v_{xy}^2 T^2}{4m}\right) \right] \quad (1)$$

where:

$$\begin{aligned} \rho_0 &= \frac{\sin(v_x X_s) \sin(v_y Y_s)}{(v_x X_s)(v_y Y_s)} \\ F &= \frac{1 + \cos \theta_1 \cos \theta_2 - \sin \theta_1 \sin \theta_2 \cos \theta_3}{\cos \theta_1 (\cos \theta_1 + \cos \theta_2)} \\ g &= \frac{2\pi\sigma_s}{\lambda} (\cos \theta_1 + \cos \theta_2) \\ v_x &= \frac{2\pi}{\lambda} (\sin \theta_1 - \sin \theta_2 \cos \theta_3), \quad v_y = \frac{2\pi}{\lambda} \sin \theta_2 \sin \theta_3 \\ v_{xy} &= \sqrt{v_x^2 + v_y^2} \end{aligned}$$

As shown in Beckmann's work, Equation 1 dictates the intensity of scattered radiation in a given observation direction based solely on the local roughness of the surface (over a relatively small area), assuming a constant incident angle. This relationship has been successfully applied to several point and line profilometry devices by examining the mean scattered power from a concentrated, coherent light source over a range of incident and observation angles. Such systems provide information regarding the local surface roughness, since the scattered light is measured from a relatively small area of the surface (Vorburger, 1990).

In this work, we accept Beckmann's treatment of the light scattering problem and its application to the measurement of local roughness. Furthermore, we extend Beckmann's scattering theory to the area-based measurement system at hand, which is capable of measuring the global surface roughness. Figure 1 depicts a two-dimensional continuous surface which can be modeled as a series of discrete surface facets, each with some given local roughness. One such facet, magnified from the continuous surface, shows the local roughness and the geometrical parameters which define the facet orientation. The surface normal,  $N$ , is shown with respect to the mean level of the facet's surface height variation. The incident and observation vectors,  $I$  and  $O$ , are shown at angles  $\theta_1$  and  $\theta_2$  from  $N$ . The direction of  $O$  is dictated by the location of the receiver in the vision system (in this case directed in the +Z direction). In addition, the global angle of incidence,  $\gamma$ , indicates the orientation of  $I$  with respect to the global horizontal. Given a fixed incident angle, the geometric parameters  $\theta_1$  and  $\theta_2$  are defined with knowledge of the surface facet's normal vector. Extending the figure into three dimensions, knowledge of the facet's normal vector would provide the parameters  $\theta_1$ ,  $\theta_2$ , and  $\theta_3$ , where  $\theta_3$  describes the tilt of the observation vector in the third dimension, just as  $\theta_2$  describes the tilt in the second dimension depicted in Fig. 1. Referring to the scattering equation, Eqn. 1, we see that the intensity of the scattered field in the known direction of

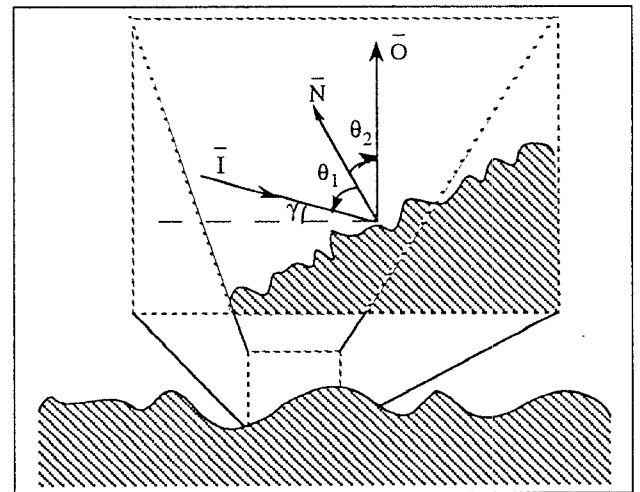


FIGURE 1 – TWO-DIMENSIONAL REFLECTION UNDER COMBINED SCATTERING/FACET MODEL

observation can be determined given  $\theta_1$ ,  $\theta_2$ , and  $\theta_3$  in addition to information about the local surface roughness of the facet. Thus, if the surface normal vector is provided for a given facet, and the local roughness and correlation distance of the facet is also known, then the mean scattered power towards the overhead vision system can be calculated for each individual facet of the surface.

In order to determine the mean scattered power from a particular facet, the scattering due to each wavelength of incident radiation must be calculated, and the resulting scattered field determined by the superposition of the scattering due to each wavelength. To do so, a new term must be provided to describe the relative contribution of each wavelength to the overall incident radiation power, since the light source used to illuminate the surface does not have constant power across the visual spectrum. The function  $C(\lambda)$  is introduced to represent the ratio of the power from a particular wavelength to the total spectral power of the incident radiation, as shown in equations 2 and 3.

$$C(\lambda_a) = \frac{P(\lambda_a)}{\int_{\lambda_{min}}^{\lambda_{max}} P(\lambda) d\lambda} \quad (2)$$

$$\int_{\lambda_{min}}^{\lambda_{max}} C(\lambda) d\lambda = 1 \quad (3)$$

The scattering equation can be integrated over the incident spectral range, resulting in

$$\Psi_{i,j} = \int_{\lambda_{min}}^{\lambda_{max}} C(\lambda) \Psi(\lambda) d\lambda \quad (4)$$

where  $\lambda_{min}$  and  $\lambda_{max}$  are the lower and upper limits of the spectrum to which the optical receiver is sensitive. Note that Eqn. 4 assumes that the global incident angle ( $\gamma$ ) is constant over the full illuminated area of the surface, which is not entirely true for the vision system at hand, since the light source is not distant enough from the surface for the incident light rays to be considered entirely parallel. However, this fact can be overlooked for the current approximation to the scattered field.

Equation 4 dictates the scattered power in the observation direction for a given facet defined by the  $i, j$  subscripts. This assumes that the facets can be identified in terms of a two-dimensional  $n \times m$  grid, where  $i$  and  $j$  are integers such that  $1 < i < n$ , and  $1 < j < m$ . This notation is convenient, as will be shown in the following discussion of appropriate surface facet dimensions. The parameters which appear in Eqn. 4 are calculated with  $\theta_2$  and  $\theta_3$  defined with the observation angle towards the vision system's CCD camera, and  $\theta_1$  defined with respect to the local  $x-y$  plane.

In order to apply Eqn. 4, appropriate dimensions for the facets must be chosen such that the continuous surface can be accurately modeled. For the present application, there is a simple choice for facet dimensions. The CCD camera used in the vision system has a resolution of  $510 \times 490$ , with each pixel in the camera receiving an amount of light reflected into the camera from a small area of the surface. It is reasonable, then, to model the surface as a  $510 \times 490$  grid of interconnected facets, with each facet scattering the light incident on the facet into a corresponding pixel in the CCD camera. This is reasonable so long as the surface area

covered by each facet is small enough compared to the global roughness of the surface. That is, the camera magnification and resolution must be sufficient so that the area of the surface which scatters light into an individual CCD pixel is smaller than about 1/2 the lower cutoff period of the global surface roughness. Using this 1/2 period criterion assures that the upper cutoff frequency of the continuous surface is modeled by the facets. In summary, the result given by Eqn. 4 rests on these assumptions:

- The global incident angle is approximately constant over the full area of the surface under inspection.
- The camera magnification and resolution are high enough so that the surface facet dimensions are smaller than 1/2 the lower cutoff period of the global surface roughness. This criterion must hold in both the  $x$  and  $y$  directions.

## DESCRIPTION OF OPTICAL SYSTEM

The photo-optical measurement method proposed here uses the apparatus shown in Figure 2. Here a sample is illuminated by a light source directed through a fiber optic cable, and a CCD camera using a high magnification lens system provides a video signal which a frame grabber converts into an 8-bit gray scale digital image at a rate of 30 frames per second. This image is then sent to a microcomputer for processing. The computer examines the light scattering pattern in the image, and calculates an optical roughness parameter, designated by  $\Omega$ , from statistical properties of the image's gray-level histogram. The  $R_a$  value for the surface is then determined through the use of a correlation curve which uniquely relates a given value of  $\Omega$  to a range of  $R_a$  values. The resulting  $R_a$  value is either displayed on a video monitor for observation or used as feedback to the machining process.

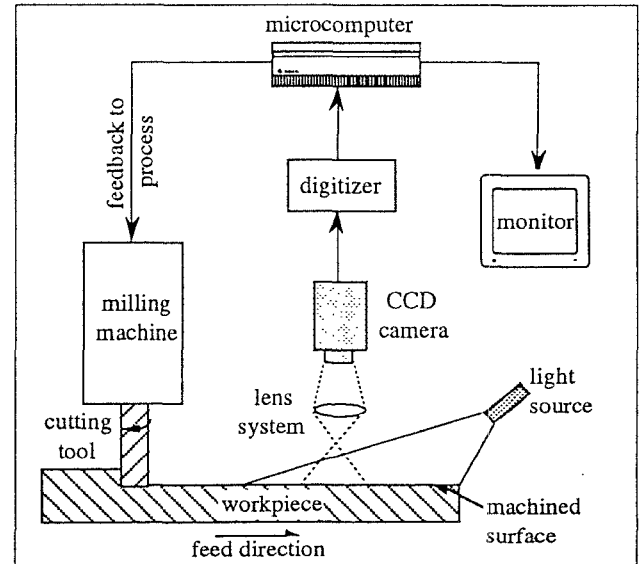


FIGURE 2 – VISION SYSTEM OPERATION

To implement the proposed optical measurement method, we designed and constructed a prototype vision system. As shown in Figure 3, a test stand (lower right) holds an aluminum sample

being measured. A fiber optic cable leads from a variable intensity light source (lower center) to the machined surface, where an adjustable fixture is used to orient the light onto the surface as required. The CCD camera at the top of the test stand sends a signal to a framegrabber within the microcomputer. Image processing software running on the computer is used to display the image and yield the optical roughness parameter for the surface on a monitor (left).

The frame grabber used in the prototype system acquires a 510x490 pixel image which reflects the activation levels of the CCD elements in the camera. This 256 gray-level image captured by the frame grabber is sent to an image processing software package for analysis. A histogram-based approach is taken to examine the image. In this approach, the gray-level of each of the pixels in the image is determined, and a frequency table for each distinct gray level (0-255) is constructed. This frequency table provides a histogram which reflects the distribution of the gray-levels in the image. A typical histogram is depicted in Figure 4.

The histogram allows the distribution of gray-levels in an image to be easily described in terms of basic statistical properties. It will be shown that the histograms of rough surfaces are often close to being normally distributed, so that the distribution can be described in terms of the mean and standard deviation of the histogram:

$$\mu = \frac{1}{n} \sum_{i=0}^{255} F_i x_i, \quad \sigma = \sqrt{\frac{1}{n} \sum_{i=0}^{255} F_i (x_i - \mu)^2} \quad (5)$$

More typically, the distribution is bounded at the low (less

bright) end, while the upper (brighter) end trails off towards zero more gradually. In this case, the histogram can be better

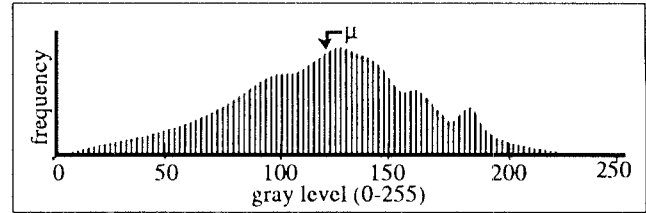


FIGURE 4 – TYPICAL GRAY-LEVEL HISTOGRAM

modeled using the two-parameter gamma distribution, which is more suitable for distributions which are bounded at one end. In practice, it seems that most histogram distributions are close enough to the normal distribution that the extra computational overhead involved with the gamma distribution is unnecessary. The optical roughness parameter ( $\Omega$ ), can be determined directly from the statistical properties of the histogram's distribution, using whatever distribution model best fits the histogram.

It has been established that the amount of light scattered into the overhead camera used in the vision system depends on the roughness of the surface, with Eqn. 4 dictating the amount of light received by an individual CCD element in the camera. Since from Eqn. 4 we know that the light received by each of the CCD elements depends directly upon the local roughness and orientation of the surface facets which comprise the surface, The

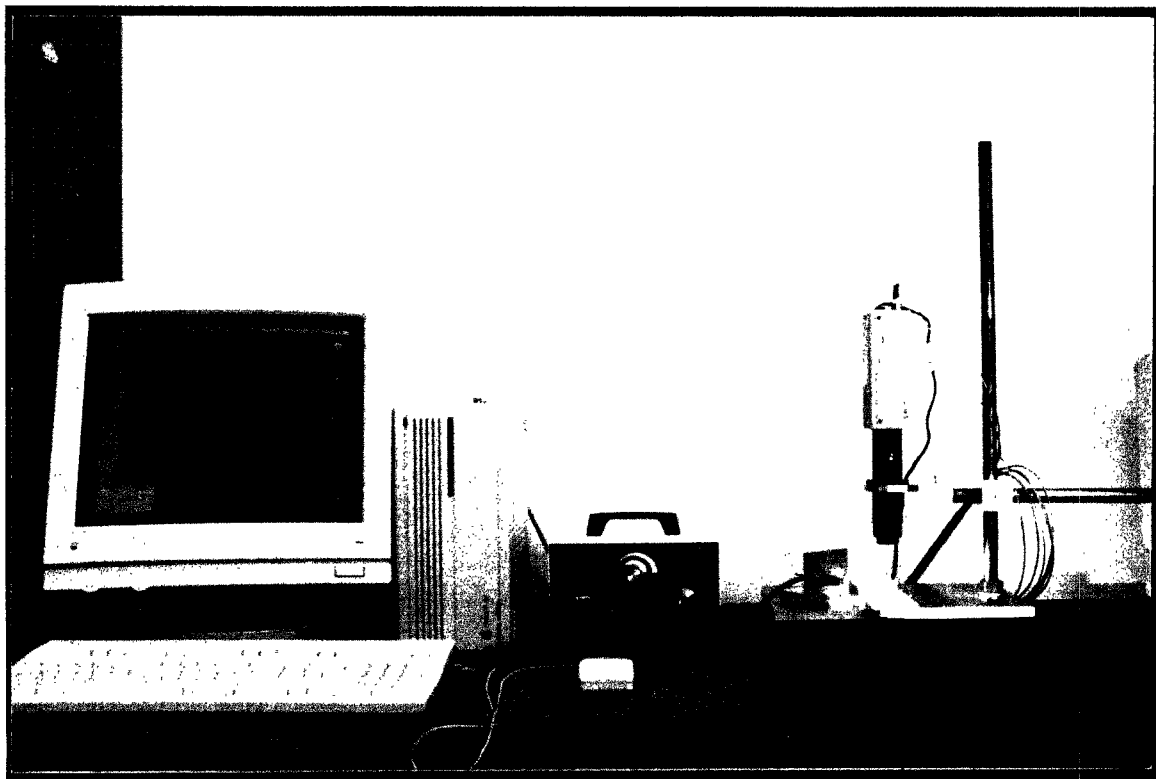


FIGURE 3 – PHOTOGRAPH OF PROTOTYPE VISION SYSTEM

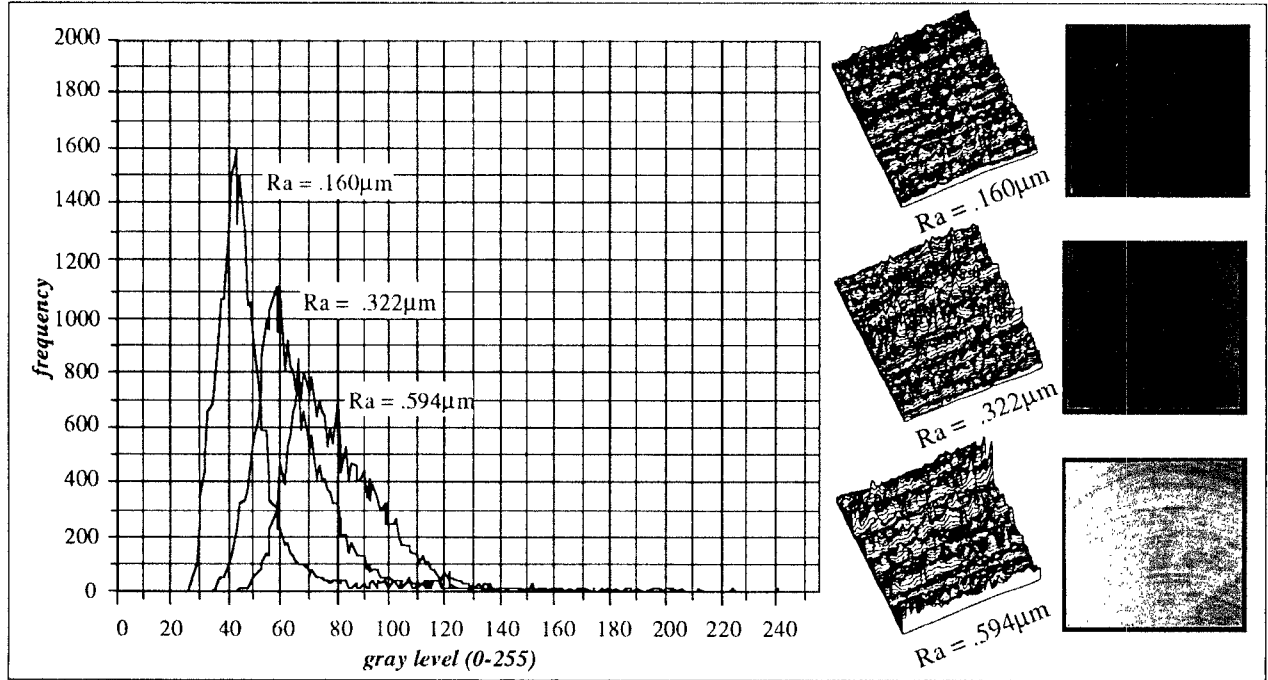


FIGURE 5 – VARIATION OF GRAY-LEVEL HISTOGRAM WITH INCREASING SURFACE ROUGHNESS

activation levels of all CCD elements in the camera will depend upon the overall global roughness of the surface.

Figure 5 shows the variation of the histogram measured from three different surfaces with roughnesses ranging from  $0.2\mu\text{m}$  -  $0.5\mu\text{m}$ . Photographs of the three surfaces are shown along with three-dimensional reconstructions of the surfaces, to provide a sense of the variation in surface topography between the surfaces. The three-dimensional reconstructions were produced by plotting the brightness level of the digital images of each surface along the z-axis. From Fig. 5, it is clear that as the roughness increases, both the mean ( $\sigma$ ) and standard deviation ( $\mu$ ) increase as well. This demonstrates that by measuring the values of  $\sigma$  and  $\mu$  for a given histogram, the roughness of the surface from which the histogram was measured can be predicted. For this reason, we propose the use of a non-dimensional index for our optical roughness parameter ( $\Omega$ ) which depends on both  $\sigma$  and  $\mu$ :

$$\Omega = \mu/\sigma \quad (6)$$

The experimental results from this work as well as from Luk (1989) and DeVoe (1992) indicate that this parameter can be successfully correlated to the actual roughness of the surface.

## EXPERIMENTAL RESULTS

### Sample Preparation

Fifty aluminum specimens were machined to  $R_a$  values ranging from  $0.15\mu\text{m}$  to  $0.60\mu\text{m}$  using a four-flute  $3/4"$  diameter end mill. The samples were machined on a Matsuura CNC Milling Center. Each of the samples was measured using a calibrated stylus profilometer at the National Institute of Standards and Technology (NIST) to determine the average roughness ( $R_a$ ) of

the surfaces. Since the surface roughness of samples machined using a milling process varies over the machining path, the roughness of each sample was determined from the average of five stylus traces over the full width of the milled path.

### Calibration

After determining the  $R_a$  value of the aluminum samples, the optical roughness parameter of each specimen was measured using the vision system, with  $\lambda = 10^\circ$  and  $\alpha = 45^\circ$ . The resulting values of  $\Omega$  were plotted against the known roughness values determined at NIST, and a curve fit was performed through the data. A third degree polynomial curve was found to provide the best fit to the experimental data, with a correlation coefficient of  $R^2 = 0.78$ . The equation of the curve is

$$\Omega = 0.316 + 47.944R_a - 48.762R_a^2 + 22.497R_a^3 \quad (7)$$

The resulting calibration curve can be used to determine the roughness of an aluminum workpiece simply by measuring the optical roughness parameter, and finding the corresponding  $R_a$  value by solving Eqn. 7.

## SENSITIVITY ANALYSIS AND DISCUSSION OF RESULTS

The performance of the vision system is effected by a broad variety of factors, ranging from environmental conditions (vibration, ambient lighting, etc.) to the repeatability of the system setup. In order to discuss the viability of utilizing the system in an industrial setting, the sensitivity of the system to these various factors must be determined. If it is found that the

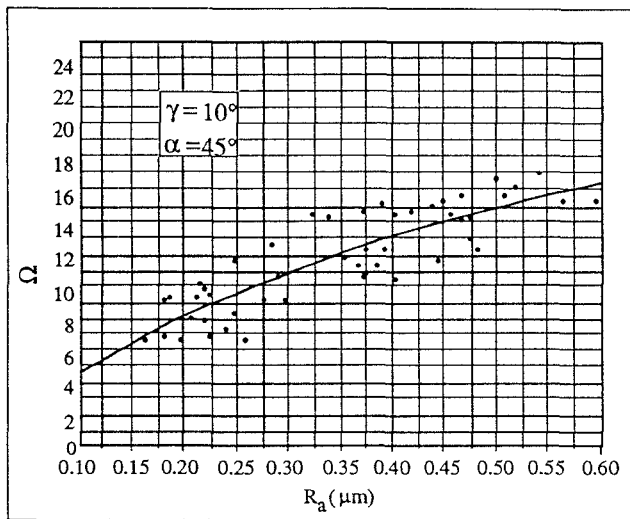


FIGURE 6 – OPTICAL CALIBRATION CURVE FOR ALUMINUM

system is especially sensitive to factors which cannot be easily measured or controlled in a machining environment, then it cannot provide accurate surface quality measurements. In order to determine the feasibility of using the system in a machining environment, the six most important factors for system performance were identified, and a full  $2^6$  factorial design was developed and instituted on the prototype vision system. The significance of the various factors was then estimated to determine the degree to which each factor effects the system performance. The factors which were assumed to be most likely to effect the system performance were determined to be:

1. environmental vibration
2. ambient lighting
3. grazing angle ( $\lambda$ )
4. light source brightness
5. horizontal light source orientation ( $\alpha$ )
6. camera magnification

The effects on system performance associated with each of these factors can be guessed at based on prior knowledge of the system and basic light-scattering theory. Environmental vibration will effect the system by causing relative motion between the vision system and the workpiece under observation, thus producing a blurring effect on the resulting image. Ambient lighting is expected to effect the measurement accuracy by shifting the mean histogram brightness level and altering the histogram's standard deviation due to the addition of secondary incident angle. According to the light scattering theory, altering the grazing angle will have a predictable effect on the optical roughness parameter, but it remains to be seen if this effect is significant enough so that a slight variation in the system setup will cause a severe change in the measurement repeatability. The light source brightness is expected to have an effect on the mean histogram level, and the degree of sensitivity to this effect must be determined. Adjusting the horizontal orientation of the vision system's camera may have a significant effect for milled surfaces, since there is a defined orientation in the surface machining marks; directing the light from different angles relative to the

machining direction may produce significantly different measurement results. Moderate changes in camera magnification may also produce large variations in system performance, although this factor is expected to be of secondary importance compared to the other five factors.

A full  $2^6$  factorial design was applied in order to determine the main effects for each of the six factors, as well as the second and third degree interaction effects. Higher order interactions were assumed to be negligible and were thus ignored in this analysis. Two levels for each factor were chosen for use in the factorial analysis. The levels were chosen to provide small to moderate variations about the normal levels of the factors. The levels were fixed as shown in Table 1:

TABLE 1 — FACTORIAL DESIGN LEVELS

DESIGN FACTOR	HIGH LEVEL	LOW LEVEL
applied vibration	off	on
ambient lighting	off	on
grazing angle	20°	10°
light source brightness	100%	80%
horizontal orientation of light	55°	45°
camera magnification	20x	30x

Environmental vibration was produced via a mechanical shaker which produced a sinusoidal excitation with a frequency of 20Hz. The shaker device was strapped to the workpiece holder during measurements, and a noticeable blurring of the captured images resulted. Ambient lighting was produced by eight 34W florescent bulbs placed between 1.5m and 3m overhead of the experimental arrangement. For the case of no ambient lighting, the only light source used to illuminate the workpiece was the fiber optic lighting integrated with the vision system. In both cases, no natural light (sunlight) was allowed to reach the workpiece. The light source brightness was measured using a simple calibrated photoresistor circuit placed at the workpiece surface in order to determine the energy incident on the surface, rather than the energy leaving the fiber optic cable, since much of the light from the cable is not directed onto the surface. The high level lighting was produced with the light source at the maximum setting (100%), and the low level was produced by reducing the light source brightness to 80% of the maximum brightness.

In order to evaluate the significance of each effect, it is necessary to estimate the experimental variation under a constant set of measurement conditions. To determine this variation, ten measurements were performed under the 'high level' conditions used in the design. The standard deviation of these ten measurements was found to be 0.0738, and the effects determined under the factorial design were compared against the natural standard deviation using a 2-sigma significance test. Those effects which are smaller than twice the standard deviation are assumed to be caused by natural variation in the measurements, and thus they do not represent true effects in the measurement process and may be ignored.

The significance of the 6 main effects, 15 second order effects (two-factor interactions), and 20 third order effects (three-factor interactions) were determined, using the estimated experimental variation to decide which effects were significant. Of the 41 total

effects, only 11 were found to be significant compared to the measured natural variation in the measurements. The factorial design yields a mathematical model of the relationship between system performance and the various effects given by

$$\Omega = \text{mean} - k_1[1] + k_2[2] + k_4[4] - k_5[5] + k_{13}[1][3] - k_{23}[2][3] + k_{24}[2][4] - k_{45}[4][5] + k_{123}[1][2][3] + k_{124}[1][2][4] - k_{235}[2][3][5] \quad (8)$$

As a preliminary examination of the empirical model given by Equation 8, each of the main effects will be discussed individually. Although we recognize the importance of examining the second and third order interaction effects, these higher order effects will be excluded from this preliminary examination.

*mean* (4.094) – The mean level in the factorial design indicates the value of  $\Omega$  which the vision system would output with each of the six factors in the design fixed at their median, or zero, level.

[1] *Ambient Lighting* ( $k_1 = -0.931$ ) – With a main effect of -0.931 when ambient lighting is reduced from normal room lighting to no lighting, it is clear that changes in ambient light has a large effect on the system performance. This presents a problem since fluctuations in ambient lighting are expected in a manufacturing environment, thus jeopardizing the accuracy of system measurements. One solution to this problem is to use the system only in an environment where the ambient lighting can be maintained at a constant level, which may not be practical in many situations. Another option is to isolate the surface being measured from all ambient light. For certain machining operations, this option may provide a reasonable solution for eliminating the effect of ambient lighting.

[2] *Grazing Angle* ( $k_2 = 0.318$ ) – As predicted by Beckmann's scattering theory, the grazing angle used in the system has a strong effect on the system performance, with a small increase in grazing angle resulting in moderate increase in the optical roughness parameter. Since the grazing angle is controllable, this effect does not present a problem for achieving consistent system performance. However, this effect implies that accuracy of the system's initial setup is critical, since a small error in the grazing angle will produce a measurable error in  $\Omega$ .

[3] *Light Source Brightness* ( $k_3 = 0$ ) – Despite the original prediction that the brightness of the fiber optic light source would have a significant effect on measurement of the optical roughness parameter, the factorial design suggests that this is not the case. While it is clear that increased brightness produces an increase in the mean histogram level, the factorial design data indicates that the standard deviation of the gray-level histogram also increases by a proportional amount, thereby leaving the optical parameter unchanged.

[4] *Horizontal Orientation* ( $k_4 = 0.977$ ) – There is a strong relationship between the horizontal orientation of the light source relative to the machining direction ( $\alpha$ ) and the system performance. This is unfortunate, since it implies that  $\alpha$  must be held constant in order to assure repeatable system

performance. This effect is suggested by light scattering theory, since milled surfaces are essentially one-dimensionally rough, or at best the superposition of several one-dimensionally rough surfaces. In a one-dimensionally rough surface, the correlation distance changes significantly with the horizontal angle at which the surface is observed. Thus, the pattern and intensity of the light scattered from the surface will vary with the horizontal orientation of the light source.

[5] *Camera Magnification* ( $k_5 = -0.159$ ) – As the camera magnification is increased a moderate amount, the optical roughness parameter is decreased a moderate amount. This may occur because as the magnification is increased, the amount of light scattered into the CCD camera is decreased due to the smaller area of the surface under observation, so that  $\mu$  is decreased. At the same time,  $\sigma$  remains unchanged, resulting in a decrease in  $\Omega$ . Since the camera magnification can be held constant, this effect is controllable.

[6] *Environmental Vibration* ( $k_6 = 0$ ) – The vibration employed during the factorial design caused a visually observable blurring of the digital image. Since a blurred image is qualitatively similar to an image with reduced resolution, it was expected that measurements performed under lateral (in-plane) vibration would yield decreased measurement accuracy. Surprisingly, the vibration was found to have no significant effect on the system performance.

The sensitivity analysis brings to light several of the positive and negative aspects of the vision system, as discussed below:

*positive aspects:*

- The vision system is unaffected by the effects of environmental vibration. Clearly, this is important attribute for any measurement system used in a manufacturing environment. Note that the vibration used in the factorial design was purely in-plane; the effects of out-of-plane vibration on system performance are uncertain.
- Changes in the brightness of the light source used to illuminate the surface do not effect the system performance. This indicates that a consumer quality light source can be used in the system, with no requirement for expensive voltage regulation for powering the light source.

*negative aspects:*

- Changes in ambient lighting can have a moderate effect on the system performance. this effect can perhaps be eliminated in most situations by maintaining the ambient lighting at a constant level, or by isolating the CCD camera and machined surface from ambient lighting entirely.
- Slight changes in the grazing angle of incident light can produce measurable errors in the optical parameter. While the grazing angle is held constant in the system operation, initial setup errors in the lighting geometry must be avoided.
- Changes in the horizontal orientation of the light source relative to the machined surface causes moderate changes in the measured optical parameter. This presents a significant problem when measuring milled surfaces, since it is difficult to maintain a constant value of  $\alpha$  in such a machining operation. This effect occurs because of the anisotropic nature of milled surfaces.



- The system performance is moderately effected by changes in camera magnification. As with the grazing angle, the camera magnification must be carefully maintained during system setup in order to assure consistent system performance.

## CONCLUSIONS

In this research, a prototype system is developed to perform surface roughness measurements using an area-based approach which is especially suitable for use as an in-process measurement technique. The results of the vision system measurements on milled aluminum surfaces demonstrate the effectiveness of the measurement technique by providing a functional calibration curve which relates the optical roughness parameter with the known surface roughness. The presented theory which dictates the pattern of light scattered into the vision system's receiver provides a starting point for understanding the operation of the system. As indicated by the results of the sensitivity analysis, the system is unaffected by the effects of in-plane workpiece vibration, which is an important characteristic for in-process sensors that is lacking from traditional contact-based profilometry techniques. The sensitivity analysis also points out the importance of baseline calibration to ensure consistent system performance, and the potential difficulties with measuring anisotropic surfaces due to a strong dependence on horizontal light orientation.

## ACKNOWLEDGMENTS

The authors wish to express their gratitude for the use of facilities and guidance by Drs. L. Ives and S. Jahanmir of the National Institute for Standards and Technology. The authors acknowledge the support of the University General Research Board, and the Institute for Systems Research at the University of Maryland at College Park under Engineering Research Centers Program: NSFD CDF 8803012.

## REFERENCES

- Beckman P, Spizzichino A., 1963, "The Scattering of Electromagnetic Waves From Rough Surfaces," Oxford:Pergamon.
- DeVoe D., Knox L., Zhang G., 1991, "Research on Surface Roughness Measurement Techniques for On-Line Machining Process Monitoring," SRC Technical Report U.G.92-1, Systems Research Center.
- DeVoe L., Duong L., Knox L., Wen J., 1992, "An Experimental Study of Surface Roughness Assessment Using Image Processing," SRC Technical Report T.R.92-28, Systems Research Center.
- DeVoe D., Knox L., Zhang G., 1992, "Active Control of Machining Processes Using Image Reconstruction and Processing," *Proceedings, 30th Annual Allerton Conference on Communication, Control, and Computing*.
- Hahn G. J. and Shapiro S. S., 1967, "Statistical Models in Engineering," John Wiley and Sons, Inc., New York.

Huynh V. M., Peticca G., 1990, "An Optical Technique for Roughness Measurement of Printing Papers," *Journal of Imaging Technology* Vol. 16, pp. 22-26.

Kerr D. E., 1951, "The Propagation of Short Radio Waves," MIT Radiation Laboratory Series No. 13, McGraw-Hill, New York.

Luk F., Huynh V., North W., 1989, "Measurement of Surface Roughness by a Machine Vision System," *Journal of Physics E: Scientific Instruments* , Vol. 22, pp. 977-80.

Rice S. O., 1951, "Reflection of Electromagnetic Waves From Slightly Rough Surfaces," *Comm. Pure Appl. Math.* Vol. 4, pp. 351-378.

Twersky V., 1957, "On the Scattering and Reflection of Electromagnetic Waves by Rough Surfaces," *Trans. I.R.E.* Vol. AP-5, pp. 81-90.

Vorburger T., Raja J., 1990, "Surface Finish Metrology," NISTIR-4088, U. S. Department of Commerce.